Reactivity of Site-Isolated Metal Clusters: Propylidyne on γ-Al_2O_3-Supported Ir_4

Andrew M. Argo, Jesse F. Goellner, Brian L. Phillips, Ghansham A. Panjabi, and Bruce C. Gates*

Contribution from the Department of Chemical Engineering and Materials Science, University of California, Davis, California 95616

Received July 31, 2000

Abstract: To contrast the reactivity of supported metal clusters with that of extended metal surfaces, we investigated the reactions of tetrairidium clusters supported on porous γ-Al_2O_3 (Ir_4/γ-Al_2O_3) with propene and with H_2. Infrared, ^{13}C NMR, and extended X-ray absorption fine-structure spectroscopy were used to characterize the ligands formed on the clusters. Propene adsorption onto Ir_4/γ-Al_2O_3 at 298 K gave stable, cluster-bound μ_3-propylidyne. Propene adsorbed onto Ir_4/γ-Al_2O_3 at 138 K reacted at approximately 219 K to form a stable, highly dehydrogenated, cluster-bound hydrocarbon species approximated as C_xH_y (such as, for example, C_3H_2 or C_2H). H_2 reacted with Ir_4/γ-Al_2O_3 at 298 K, forming ligands (likely hydrides), which prevented subsequent reaction of the clusters with propene to form propylidyne. Propylidyne on Ir_4 was stable in helium or H_2 as the sample was heated to 523 K, whereupon it reacted with oxygen of the support to give CO. Propylidyne on Ir_4 did not undergo isotopic exchange in the presence of D_2 at 298 K. In contrast, the literature shows that propylidyne chemisorbed on extended metal surfaces is hydrogenated in the presence of H_2 (or D_2) and exchanges hydrogen with gaseous D_2 at room temperature; in the absence of H_2, it decomposes thermally to give hydrocarbon fragments at temperatures much less than 523 K. The striking difference in reactivities of propylidyne on clusters and propylidyne on extended metal surfaces implies the requirement of ensembles of more than the three metal surface atoms bonded to propylidyne in the surface reactions. The results highlight the unique reactivity of small site-isolated metal clusters.

Introduction

Metals in technological catalysts are usually dispersed as small, nonuniform clusters or crystallites (particles) on high-area porous supports. Models of these catalysts range from size-selected gas-phase metal clusters to single crystals of metal. Our goals were to investigate a more realistic model of a metal catalyst, well-defined clusters isolated on a support, namely, Ir_4 on γ-Al_2O_3. The sample was prepared by adsorption of $[Ir_4(CO)_{12}]$ onto γ-Al_2O_3, giving $[Ir_4(CO)_{12}]/\gamma$-Al_2O_3, which was decarbonylated to give nearly monodisperse Ir_4/γ-Al_2O_3.

Of the model catalysts used to investigate fundamentals of metal catalysis, the most thoroughly investigated are single crystals, which offer the advantages of stability, structural simplicity, and ease of characterization by the methods of surface science. An example of a well-characterized single-crystal catalyst is Pt(111), which is used for hydrogenation of alkenes; sum frequency generation has been applied to observe intermediates on the surface during the catalysis.[1−4] Disadvantages of single crystals as model catalysts are that the large periodic arrays of metal atoms have properties different from those of isolated clusters and that, furthermore, single crystals cannot be used to determine the influence of a support.

Here we report results characterizing reactions on supported metal clusters that lend themselves to comparison to results characterizing single crystals of metal. Infrared, extended X-ray absorption fine structure (EXAFS), and ^{13}C NMR spectroscopy were used to identify species formed by the reactions of propene and of H_2 with Ir_4 on γ-Al_2O_3.

Experimental Section

Materials, Sample Preparation, and Handling. The synthesis of Ir_4/γ-Al_2O_3, described elsewhere,[5] was carried out on a vacuum line or in a drybox (Vacuum Atmospheres HE-63-P) purged with N_2 that was recirculated through O_2- and moisture-scavenging traps (supported Cu particles and zeolite 4A, respectively). The drybox was equipped with O_2 and moisture detectors, indicating concentrations <2 ppm. Reagent grade *n*-pentane solvent (Aldrich) was dried over sodium benzophenone ketyl. He (Matheson, 99.999%) and propene (Matheson, 99.5%) were purified by passage through traps to remove traces of O_2 and moisture. H_2 was supplied by Matheson (99.999%) or generated by electrolysis of water in a Balston generator (99.99%) and purified by traps. $[Ir_4(CO)_{12}]$ (Strem, 98%) was used as received. γ-Al_2O_3 powder (Aluminum Oxide C, Degussa) was made into a paste by adding deionized water, followed by drying overnight at 393 K. It was then ground and stored in a drybox. ^{13}C-enriched propene (1,2,3-$^{13}C_3$, 99%) was provided by Cambridge Isotope Laboratories. The standard Ir_4/γ-Al_2O_3 samples contained 1 wt % Ir. A few samples containing 4 wt % Ir were used for spectroscopic measurements when signal-to-noise ratios would otherwise have been low.

X-ray Absorption Spectroscopy. X-ray absorption experiments were performed on beamline X-11A of the National Synchrotron Light Source (NSLS) at Brookhaven National Laboratory, Upton, NY, and

(1) Cremer, P. S.; Su, X.; Shen, Y. R.; Somorjai, G. A. *Catal. Lett.* **1996**, *40*, 143.
(2) Cremer, P. S.; Su, X.; Shen, Y. R.; Somorjai, G. A. *J. Phys. Chem.* **1996**, *100*, 16302.
(3) Cremer, P. S.; Somorjai, G. A. *J. Chem. Soc., Faraday Trans.* **1995**, *91*, 3671.
(4) Cremer, P. S.; Su, X.; Shen, Y. R.; Somorjai, G. A. *J. Am. Chem. Soc.* **1996**, *118*, 2942.
(5) Alexeev, O.; Panjabi, G.; Gates, B. C. *J. Catal.* **1998**, *173*, 196.

10.1021/ja002818q CCC: $20.00
Published on Web 02/17/2001

Table 1. EXAFS Fit Parameters Characterizing $[Ir_4(CO)_{12}]/\gamma\text{-}Al_2O_3$ Treated in Flowing Helium at 588 K and Scanned at a Pressure of $<10^{-5}$ Torr[a]

	temp of scan, K							
	77				298			
backscatterer	N	R [Å]	$\Delta\sigma^2 \cdot 10^3$ [Å^2]	ΔE_0 [eV]	N	R [Å]	$\Delta\sigma^2 \cdot 10^3$ [Å^2]	ΔE_0 [eV]
Ir	3.3	2.66	4.8	−4.3	3.4	2.65	6.2	−4.1
Al	0.3	1.57	5.0	12.8	0.5	1.56	6.3	9.1
C	0.4	1.91	−3.5	3.6	0.5	1.90	−3.5	−1.1
O	0.4	2.06	1.3	−4.9	0.7	2.03	5.5	−1.4
O	1.2	2.56	1.8	−9.2	1.2	2.56	1.8	−9.2

[a] Notation: N, coordination number; R, absorber−backscatterer distance; $\Delta\sigma^2$, Debye−Waller factor; and ΔE_0, inner potential correction. The approximate experimental uncertainties are as follows: N, coordination number (±10%); interatomic distance, r (±0.02 Å); Debye−Waller factor, $\Delta\sigma^2$ (±20%); and inner potential correction, ΔE_0 (±20%).[17]

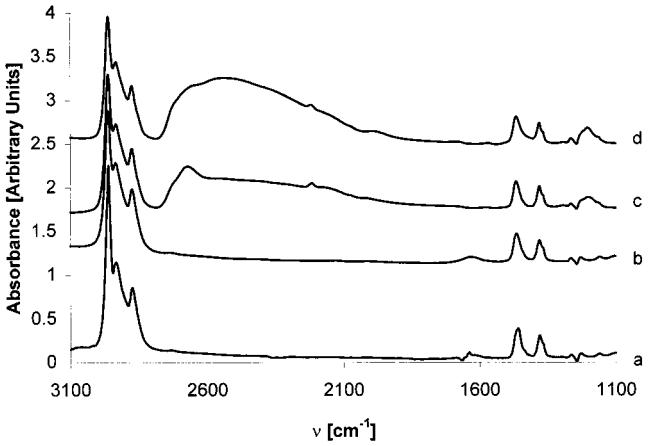

Figure 1. Infrared difference spectra (relative to sample under flow of He) for sequential treatment of $Ir_4/\gamma\text{-}Al_2O_3$ at 298 K with a, C_3H_6; b, He; c, D_2; and d, He.

on beamline 2-3 of the Stanford Synchrotron Radiation Laboratory (SSRL) at the Stanford Linear Accelerator Center, Stanford, CA. The storage ring electron energy was 2.5 GeV at NSLS and 3 GeV at SSRL; the beam current was 140−240 mA at NSLS and 50−100 mA at SSRL. Samples for transmission EXAFS experiments were prepared in dryboxes at the synchrotrons. To verify the synthesis of $Ir_4/\gamma\text{-}Al_2O_3$, the sample was pressed into a self-supporting wafer, loaded, and sealed into an EXAFS cell within the drybox and then scanned under vacuum at approximately liquid nitrogen temperature. A homemade EXAFS cell consisting of a variable-temperature stainless steel body sealed with Mylar windows (Supporting Information, Figure 1) was used for samples in the presence of flowing treatment gases. Higher harmonics in the X-ray beam were minimized by detuning the Si(111) double-crystal monochromator at NSLS or the Si (220) monochromator at SSRL by 20−25% at the Ir L_{III} edge (11 215 eV).

Infrared Spectroscopy. Transmission spectra were recorded with a Bruker IFS-66v spectrometer having a spectral resolution of 4 cm^{-1}. Samples were pressed into self-supporting wafers and loaded into the cell in the drybox. The cell (In-situ Research Institute, Inc., South Bend, IN) used in flow experiments allowed for measurement of transmission spectra while treatment gases flowed over and through the wafer at temperatures ranging from 298 to 573 K. Low-temperature adsorption experiments were carried out with a liquid-nitrogen-cooled cell.[6] The wafer was cooled to approximately 140 K, treatment gases were dosed into the cell, and the wafer was allowed to warm over a period of several hours as spectra were recorded. Each sample was scanned 128−512 times and the signal averaged. Difference spectra were calculated by subtracting the spectrum of the sample in the presence of an inert gas (typically helium) from that of the sample in the treatment gas. When the absorption by the treatment gas was significant, the spectrum of the treatment gas was subtracted from that of the sample in the treatment gas.

^{13}C NMR Spectroscopy. MAS-NMR spectra were recorded using a Chemagnetics CMX-400 spectrometer at a frequency of 100.63 MHz for ^{13}C. Samples in the drybox were loaded into 7.5-mm-o.d. ZrO_2 rotors and sealed with double-O-ring-sealed PTFE plugs. Samples were rotated at rates from 3.3 to 4.5 kHz at the magic angle (54.4° relative to the magnetic field). Variation of the rotation rate allowed identification of spinning sidebands.

Kinetics of Adsorption. A RMX-100 multifunctional catalyst-testing and -characterization system (Advanced Scientific Design, Inc., Grosse Pointe Park, MI) with a vacuum capability of 10^{-8} Torr was used for chemisorption experiments. Adsorption kinetics were determined by measuring the volume of treatment gas adsorbed as a function of time on an ∼0.25-g sample in a 10-mL glass sample holder. The sample container was evacuated, and then a known volume of gas was dosed into the sample container, which was sealed immediately. The resulting pressure of gas in contact with the sample was monitored as a function of time. Chemisorbed species were distinguished from physisorbed species by the results of two consecutive adsorption experiments with the sample, separated by 30 min of evacuation (10^{-6} to 10^{-7} Torr), the data quantifying both chemisorbed and physisorbed species.

Hydrogen Chemisorption Capacities. Adsorption isotherms were measured at 298 K, as described elsewhere.[5] Hydrogen chemisorption capacities were measured for $Ir_4/\gamma\text{-}Al_2O_3$ with and without propene pretreatment. For comparison, hydrogen chemisorption capacities of $\gamma\text{-}Al_2O_3$ were also measured with and without propene pretreatment.

Data Analysis

X-ray Absorption Spectra. EXAFS data were analyzed using experimentally and theoretically determined reference files, the former obtained from EXAFS data characterizing materials of known structure (Supporting Information, Table 1). Preparation of the EXAFS reference files is described separately,[7−11] as are the details of the analysis procedures.[11−13]

Kinetics of Adsorption. Adsorption rate parameters for postulated adsorption models[14,15] were determined by nonlinear least-squares regression.[16]

Results

EXAFS Evidence of Ir_4 Tetrahedra on $\gamma\text{-}Al_2O_3$. EXAFS parameters characterizing the sample formed by adsorption of $[Ir_4(CO)_{12}]$ onto amorphous $\gamma\text{-}Al_2O_3$ powder (calcined at 673 K), followed by decarbonylation in flowing helium at 573 K

(6) De La Cruz, C.; Sheppard, N. *J. Chem. Soc., Faraday Trans*. **1997**, *93*, 3569.
(7) Duivenvoorden, F. B. M.; Koningsberger, D. C.; Uh, Y. S.; Gates, B. C. *J. Am. Chem. Soc*. **1986**, *108*, 6254.
(8) Lu, D.; Rehr, J. J. *J. Phys. (Paris) C8* **1986**, *47*, 67.
(9) van Zon, F. B. M.; Maloney, S. D.; Gates, B. C.; Koningsberger, D. C. *J. Am. Chem. Soc*. **1993**, *115*, 10317.
(10) van Zon, J. B. A. D., Ph.D. Dissertation, Eindhoven University of Technology, The Netherlands, 1988.
(11) van Zon, J. B. A. D.; Koningsberger, D. C.; van't Blik, H. F. J.; Sayers, D. E. *J. Chem. Phys*. **1985**, *82*, 5742.
(12) Vaarkamp, M.; Linders, J. C.; Koningsberger, D. C. *Phys. B* **1995**, *209*, 159.
(13) Kirlin, P. S.; van Zon, F. B. M.; Koningsberger, D. C.; Gates, B. C. *J. Phys. Chem*. **1990**, *94*, 8439.

Table 2. EXAFS Fit Parameters Characterizing Ir_4/γ-Al_2O_3 under Flow of Treatment Gas at 298 K and a Pressure of 760 Torr[a]

	treatment gas											
	helium				propene				H_2			
backscatterer	N	R [Å]	$\Delta\sigma^2\cdot10^3$ [Å^2]	ΔE_0 [eV]	N	R [Å]	$\Delta\sigma^2\cdot10^3$ [Å^2]	ΔE_0 [eV]	N	R [Å]	$\Delta\sigma^2\cdot10^3$ [Å^2]	ΔE_0 [eV]
Ir	2.8	2.63	4.6	0.0	2.8	2.64	4.7	−3.3	3.3	2.66	6.1	−4.7
Al									0.3	1.65	7.5	−3.2
Al	1.6	3.52	0.1	5.4	1.9	3.55	1.7	3.1	0.6	3.21	3.3	−4.2
C	0.7	1.80	0.7	17.8	0.5	1.80	1.2	20.0				
O	0.5	2.06	−1.9	4.2	0.6	2.06	−0.3	5.1	0.2	2.15	−2.7	−3.6
O	1.5	2.60	7.1	−8.3	1.1	2.69	3.8	−11.1	1.4	2.66	−1.2	−5.6

[a] Notation as in Table 1.

Table 3. Infrared Assignments for the Sample Formed from Propene Adsorption on Ir_4/γ-Al_2O_3 at 298 K and 760 Torr and the Vibrational Spectra of Propylidyne Ligands on Surfaces and Related Pure Compounds

	assignment, cm^{-1}										
sample	$\nu_{as}(CH_3)$	$\nu_s(CH_2)$	$\nu_s(CH_3)$	$\delta_{as}(CH_3)$	$\delta_s(CH_2)$	$\delta_s(CH_3)$	CH_2 wag + ν(CC)	$\rho(CH_3)$	ν(CC)	CH_3 rock	ref
CH_3CH_2C on Ir_4/γ-Al_2O_3	2961	2934	2874	1465	1380	1365	not obsd[a]	1161	not obsd[a]	not obsd[a]	this work
CH_3CH_2C on Pt/SiO_2	2960	2920	2860	1465	1410	1365					25
				1450		1355					
CH_3CH_2C on Pt/SiO_2	2960	2920	2860	1450	1410	1365					24
CH_3CH_2C on Pt(111)	2961	2921	2865	1450	1407		1303		1103	1055	24
									929	1039	
CH_3CH_2C on Rh(111)				1445		1385	1290	1120	1055	1055	23
$Cl_3CCH_2CH_3$				1455	1430	1382	1323	1107	1066		80
$Co_3(CO)_9(C_3H_5)$				1450	1420	1370		1155	1050		26

[a] The absorption in this portion of the infrared spectrum is dominated by the alumina support, making the identification of propylidyne modes in this region difficult.

for 2 h, specifically including the Ir−Ir first shell coordination number of about 3 (Table 1), are consistent with the expected[5] site-isolated tetrahedral Ir_4. EXAFS spectra of Ir_4/γ-Al_2O_3 in flowing helium, propene, or H_2 at 298 K and 760 Torr (Table 2) show that the tetrahedral metal frame remained unchanged within the experimental uncertainty.[17,18,22] The EXAFS data also show Ir−Al, Ir−O, and Ir−C contributions. The former two indicate cluster attachment to the γ-Al_2O_3 support.[5] The Ir−C contribution indicates residual carbon on the clusters from the decomposition of CO during the decarbonylation step or from hydrocarbon species formed from the adsorption of propene onto the clusters.

Infrared Evidence of Ligands Bonded to Ir_4 Supported on γ-Al_2O_3. Contacting of Ir_4/γ-Al_2O_3 with propene at 298 K and 760 Torr gave a sample with infrared modes at 2961, 2934, 2874, 1635, 1465, 1380, 1365, 1265, 1230, and 1161 cm^{-1} (Figure 1, spectrum a). To resolve individual surface species, spectra resulting from dosing of different amounts of propene onto Ir_4/γ-Al_2O_3 at 298 K were recorded (Figure 2). The modes at 2961, 2934, 2874, 1465, 1380, 1365, and 1161 cm^{-1} are attributed to a single species, because they occurred in constant ratios of intensities and separately from other modes. Comparison of this part of the spectrum to the vibrational spectra of propylidyne on Rh(111),[23] Pt(111),[24] and Pt particles dispersed on SiO_2 (Pt/SiO_2)[24,25] and that of reference metal cluster compounds with propylidyne ligands[26] (Table 3) leads to the identification of μ_3-propylidyne on Ir_4/γ-Al_2O_3; we thus refer

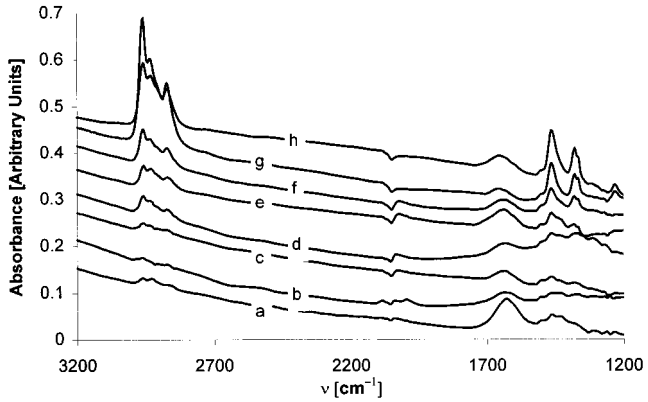

Figure 2. Infrared difference spectra (relative to freshly decarbonylated sample) of Ir_4/γ-Al_2O_3 dosed with propene in the following ratios of C_3H_6/Ir_4: a, 1; b, 2; c, 4; d, 8; e, 20; f, 81; g, 162; and h, 402.

(14) Dissociative adsorption kinetics: $r_{ads} = k_{ads}P_{H_2}(n_{tot} - n_{ads})^2$, where r_{ads} is the rate of chemisorption [mol g^{-1} s^{-1}]; k_{ads}, the chemisorption rate constant [g s^{-1} $Torr^{-1}$ mol^{-1}]; P_{H_2}, the H_2 pressure [Torr]; n_{tot}, the number H atoms adsorbed at equilibrium [mol g^{-1}]; and n_{ads}, the number of H atoms adsorbed [mol g^{-1}].

(15) Molecular adsorption kinetics: $r_{ads} = k_{ads}\,P_{H_2}\,(n_{tot} - n_{ads})$, where the terminology matches that of footnote (14), with the exception of k_{ads}, the chemisorption rate constant [s^{-1} $Torr^{-1}$].

(16) Goodness of fit of the hydrogen chemisorption rate models was determined by the correlation factors for the plot of the predicted chemisorption rate, with regressed rate parameters, against the experimental chemisorption rate.

(17) Vaarkamp, M. *Catal. Today* **1998**, *39*, 271.

(18) The importance of anharmonic contributions to the EXAFS spectra of Ir_4/γ-Al_2O_3 during in-situ experiments was investigated qualitatively by scanning a wafer form of the sample at 77 and 298 K under vacuum.[12,19−21] The results show negligible differences between the fit parameters from the data that were obtained at 77 and 298 K (other than the Debye−Waller factors), which implies that the anharmonic vibrational contributions to the EXAFS spectra recorded at 298 K were negligibly small.

(19) Crozier, E. D.; Seary, A. J. *Can. J. Phys.* **1980**, *58*, 1388.

(20) Crozier, E. D. *Physica B* **1995**, *208* & *209*, 330.

(21) Stern, E. A.; Līviņš, P.; Zhang, Z. *Phys. Rev. B* **1991**, *43*, 8850.

(22) The approximate experimental uncertainties in the EXAFS parameters are the following: N, coordination number (±10%); interatomic distance, r (±0.02 Å); Debye−Waller factor, $\Delta\sigma^2$ (±20%); and edge energy shift, E_0 (±20%).[17]

(23) Bent, B. E.; Mate, C. M.; Crowell, J. E.; Keol, B. E.; Somorjai, G. A. *J. Phys. Chem.* **1987**, *91*, 1493.

(24) Chesters, M. A.; De La Cruz, C.; Gardner, P.; McCash, E. M.; Pudney, P.; Shahid, G.; Sheppard, N. *J. Chem. Soc., Faraday Trans.* **1990**, *86*, 2757.

(25) Shahid, G.; Sheppard, N. *Spectrochim. Acta* **1990**, *46A*, 999.

(26) Seyferth, D.; Rudie, C. N.; Merola, J. S. *J. Organomet. Chem.* **1978**, *162*, 89.

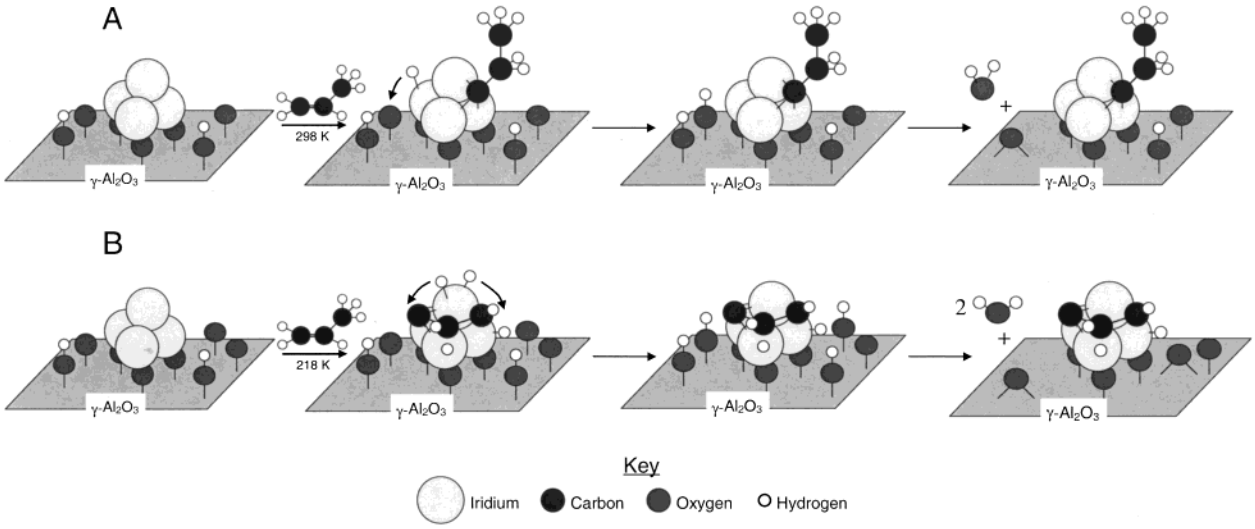

Figure 3. Schematic representation of the formation of propylidyne on $Ir_4/\gamma\text{-}Al_2O_3$.

Table 4. Infrared Spectra of C_3H_6 in the Gas Phase and Adsorbed on $Ir_4/\gamma\text{-}Al_2O_3$ at 138 K

	assignment, cm^{-1}												
sample	$\nu_{as}(CH_2)$	$\nu(CH)$	$\nu_s(CH_2)$	$\nu_{as}(CH_3)$	$\nu_{as}(CH_3)$	$\nu_s(CH_3)$	$\nu(C{=}C)$	$\delta_{as}(CH_3)$	$\delta(CH_2)$	$\delta(CH_3)$	$\delta(CH)$	$\rho(CH_2)$	$\rho(CH_3)$
C_3H_6 gas[31]	3081	3012	2979	2960	2916	2852	1647	1472	1416	1399	1287	1224	1043
								1448				1166	996
C_3H_6 adsorbed on $Ir_4/\gamma\text{-}Al_2O_3$[a]	3077	3014	2976	2968		2859	1640	1458	1415	1376	1296	1170	1049
								1442					1007
C_3H_6 adsorbed on $Ir_4/\gamma\text{-}Al_2O_3$[b]			2922		2954	2875		1474	1445	1378			
di-σ-bonded propene adsorbed on Pt/SiO_2[24]			2920		2950	2880		1450	1425	1355			

[a] Propene adsorbed at 138 K and scanned at 138 K. [b] Propene adsorbed at 138 K and warmed to 243 K.

to the supported organometallic cluster as $CH_3CH_2CIr_4/\gamma\text{-}Al_2O_3$. The stoichiometry of the propylidyne formation is inferred to be as follows

$$C_3H_6 + Ir_4/\gamma\text{-}Al_2O_3 \rightarrow CH_3CH_2CIr_4/\gamma\text{-}Al_2O_3 + H \quad (1)$$

(the hydrogen that is produced reacts, at least in part, with the $\gamma\text{-}Al_2O_3$ support; see below). This reaction is represented schematically in Figure 3A.

A second organometallic cluster species is associated with the modes at 1265 and 1230 cm^{-1}, which were observed at low intensity for low propene exposures (<4.0 C_3H_6/Ir_4), when propylidyne formation did not occur (Figure 2, spectra a−c). These modes were absent for propene exposures in the range of $8.0 < C_3H_6/Ir_4 < 81$ (Figure 2, spectra d−f)—when propylidyne was formed predominantly—and they were observed along with the propylidyne modes at high propene exposures ($C_3H_6/Ir_4 > 162$) (Figure 2, spectra g−h). The identities of the species associated with these modes are addressed below.

The remaining mode, at 1635 cm^{-1}, is identified as the O−H bending frequency of water on the $\gamma\text{-}Al_2O_3$ support, because it was observed when water was adsorbed onto $\gamma\text{-}Al_2O_3$[27] or $Ir_4/\gamma\text{-}Al_2O_3$ (Supporting Information, Figure 2). This mode occurred simultaneously with the formation of either propylidyne or, at greater intensity, the second organometallic cluster species mentioned in the preceding paragraph. These results indicate that at least part of the hydrogen formed in the dissociation of propene on Ir_4 was spilled over[28] onto the support, where it reacted to form surface OH groups and water, as represented schematically in Figures 3A and B.

The second supported organometallic cluster species referred to above (associated with the modes at 1230 and/or 1265 cm^{-1}) occurred in association with large increases in the amount of water on the support; thus, the hydrocarbon ligands are inferred to be highly dehydrogenated species that are formed from propene. These frequencies nearly match the C−C stretching frequency observed[29] for a species approximated as C_2H on a metal single crystal, Ir(111) (1260 cm^{-1}); thus, we refer to the dehydrogenated species as approximately C_xH_y (e.g., C_3H_2[30] or C_2H[23,29]). The stoichiometry of the formation of C_xH_y (for example, $x = 3$) is inferred to be as follows:

$$C_3H_6 + Ir_4/\gamma\text{-}Al_2O_3 \rightarrow C_3H_yIr_4/\gamma\text{-}Al_2O_3 + (6 - y)H \quad (2)$$

(where, again, the hydrogen is spilled over, at least in part, onto the support).

When propene was brought in contact with $Ir_4/\gamma\text{-}Al_2O_3$ at a low temperature (138 K) and the sample warmed slowly, the propene initially adsorbed molecularly, as shown by the similarity of the infrared spectrum (Figure 4) to that of gaseous propene[31] (Table 4). As the sample warmed, adsorbed propene modes began decreasing in intensity at 198 K and were completely removed at approximately 218 K. As propene was converted and these modes disappeared, a very strong support surface water peak arose at 1635 cm^{-1}, along with a less intense peak for C_xH_y at 1266 cm^{-1}. The results indicate that at temperatures above 219 K, adsorbed propene was converted to C_xH_y, as shown schematically in Figure 3B. Neither continued

(27) Peri, J. B.; Hannan, R. B. *J. Phys. Chem.* **1960**, *64*, 1526.
(28) Conner, W. C., Jr.; Falconer, J. L. *Chem. Rev.* **1995**, *95*, 759.
(29) Marinova, T. S.; Kostov, K. L. *Surf. Sci.* **1987**, *181*, 573.
(30) Avery, N. R.; Sheppard, N. *Proc. R. Soc. London A* **1986**, *405*, 1.
(31) Shimanouchi, T. Tables of Molecular Vibrational Frequencies, Vol. I NSRDS−NSB 39, Vol. II *J. Chem. Ref. Data* **1977**, *6*, 993.

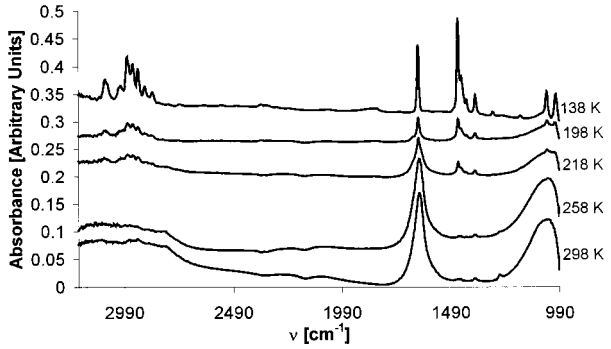

Figure 4. Infrared difference spectra (relative to sample under vacuum) of low-temperature C_3H_6 adsorption on Ir_4/γ-Al_2O_3 and the resulting spectra as the sample was warmed to room temperature.

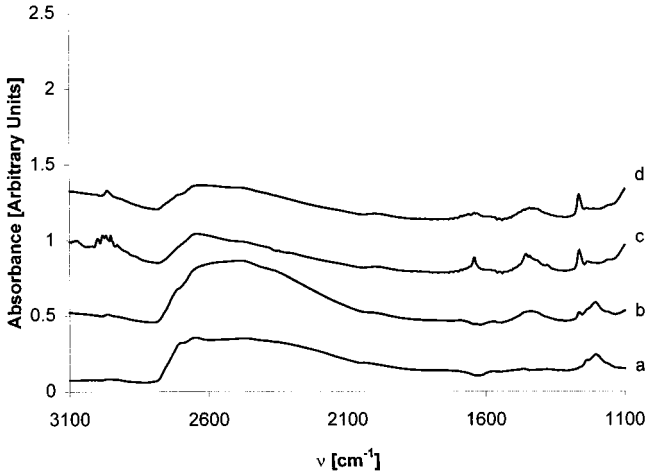

Figure 5. Infrared difference spectra (relative to sample under flow of He) for sequential treatment of Ir_4/γ-Al_2O_3 at 298 K with a, D_2; b, He; c, C_3H_6; and d, He.

warming of the sample to 298 K nor additional exposure of the warmed sample to propene at 298 K and 760 Torr resulted in the formation of additional modes. This last observation indicates that C_xH_y remained on the clusters.

When propene was allowed to react at 298 K and 760 Torr with Ir_4/γ-Al_2O_3 that had been pretreated with H_2 or D_2 (at 298 K and 760 Torr), infrared modes corresponding to propylidyne were observed, but with much lower intensities (Figure 5, spectrum d) than when freshly decarbonylated Ir_4/γ-Al_2O_3 was used (Figure 1, spectrum a). These results indicate that H_2 or D_2 formed species that hindered formation of propylidyne from propene on Ir_4. Instead, propene was mainly converted into C_xH_y, as indicated by the infrared mode at 1265 cm^{-1} (Figure 5, spectrum d).

^{13}C NMR Evidence of Propylidyne on Ir_4/γ-Al_2O_3. The single-pulse ^{13}C MAS-NMR spectrum of the sample that was formed by contacting isotopically enriched propene (1,2,3-$^{13}C_3$, 99%) with Ir_4/γ-Al_2O_3 at 298 K and 50 Torr includes resonances[32] at 7.7, 11.7, 13.8, 17.5, 19.4, 22.0, 27.0, 28.7, 112 (rotor), 134, and 165 ppm (Figure 6). The cross-polarization (CP) ^{13}C MAS-NMR spectrum of this sample includes resonances at 7.4, 12.8, 18.1, 27.0, 134, and 186 ppm (Figure 6). The resonances at 22−27 ppm are associated with species formed by adsorption of propene onto the γ-Al_2O_3 support.[33,34]

(32) The listed resonances do not include spinning sidebands.

(33) The ^{13}C MAS-NMR spectra of the species formed by adsorption of propene onto γ-Al_2O_3 at 298 K and 50 Torr resulted in peaks at 21.7 and 25.8 ppm (Supporting Information, Figure 5).

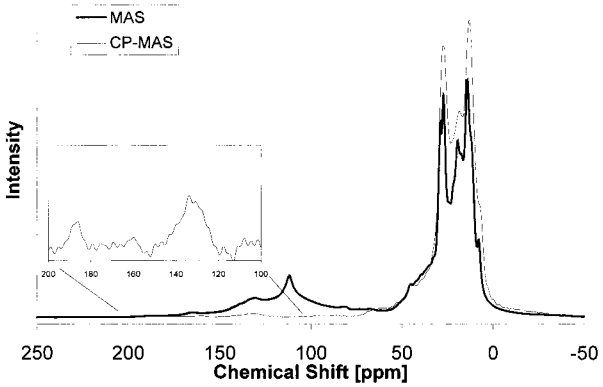

Figure 6. ^{13}C NMR spectra of $^{13}C_3H_6$ adsorbed onto Ir_4/γ-Al_2O_3 at 298 K and 100 Torr (forming propylidyne). MAS data were obtained at 100.6 MHz with a 4.4 kHz spinning rate, 6-μs pulse width, and 15-s relaxation time. CP-MAS data were obtained at 100.6 MHz with a 4.0 kHz spinning rate and 5-ms contact time.

Table 5. ^{13}C NMR Assignments of Propylidyne and C_xH_y on Ir_4/γ-Al_2O_3

	chemical shift, ppm	
assignment	C_xH_y on Ir_4/γ-Al_2O_3	ref material[35]
$-CH_2-$	7.4, 12.8	−5 to 15[a]
$-CH_3$	18.1	13−26[a]
$-C\equiv$	186.0	219.3,[b] 154.7[c]
C_xH_y	132	134.4[d]

[a] Ethyl ligands of transition metal complexes. [b] $[Ru_3(CO)_9(\mu\text{-}H)_3(\mu_3\text{-}CCH_3)]$. [c] $[Os_3(CO)_9(\mu\text{-}H)_3(\mu_3\text{-}CCH_3)]$. [d] $[Os_3(CO)_9(\mu\text{-}H)(\mu_3\text{-}\eta^2\text{-}CCH)]$.

The other resonances are attributed to the species that were formed from propene and bonded to Ir_4. These agree well with the resonances in the ^{13}C NMR spectra of osmium clusters and ruthenium clusters incorporating ethylidyne ligands and osmium clusters incorporating C−CH ligands (Table 5). The identities of both alkylidyne ligands and C_xH_y ligands in the NMR sample are confirmed by the infrared spectrum (Supporting Information, Figure 3).

Infrared Evidence of the Stability of Ligands Bonded to Ir_4 on γ-Al_2O_3. Propylidyne and C_xH_y, produced together on Ir_4/γ-Al_2O_3 by adsorption of propene at 298 K and 760 Torr, were stable in flowing helium at 298 K and 760 Torr, as shown by the infrared spectra (Figure 1, spectrum b). These species did not undergo exchange with C_3D_6 gas at 298 K and 50 Torr (Supporting Information, Figure 4). Propylidyne and C_xH_y species were unmodified in 100 Torr of D_2 at 298 K (Figure 1, spectrum c), although hydrogen in O−H groups of the support and support water readily underwent isotopic exchange,[36] as expected.[37]

$CH_3CH_2CIr_4/\gamma$-Al_2O_3 was stable during heating in flowing helium (Figure 7A) or H_2 (Figure 7B) at temperatures up to 523 K, and it was still present at 573 K. At temperatures between 523 and 573 K, infrared modes indicating CH_3CH_2C were replaced by very broad modes in the range of 1800 and 2200

(34) Samples incorporating Ir_4 took up 2 orders of magnitude more propene than the support alone (Supporting Information, Figure 7).

(35) Evans, J.; McNulty, G. S. *J. Chem. Soc., Dalton Trans.* **1984**, 79.

(36) Hydrogen in water on the surface of γ-Al_2O_3 was exchanged with deuterium, as shown by the replacement of δ_{OH} at 1635 cm^{-1} with δ_{OD} at 1204 cm^{-1} and the replacement of ν_{OH} at ∼3300 cm^{-1} with ν_{OD} at ∼2400 cm^{-1}. Surface hydroxyl groups of γ-Al_2O_3 were converted to deuterioxyl groups of γ-Al_2O_3, as shown by the replacement of ν_{OH} at 3600−3800 cm^{-1} with ν_{OD} at 2600−2800 cm^{-1}.

(37) Carter, J. L.; Lucchesi, P. J.; Corneil, P.; Yates, D. J. C.; Sinfelt, J. H. *J. Phys. Chem.* **1965**, *69*, 3070.

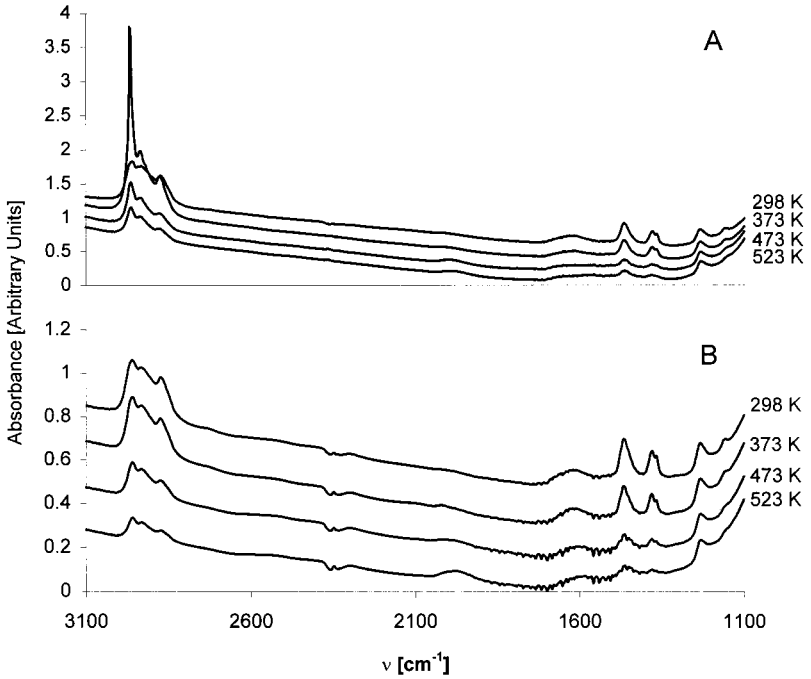

Figure 7. Infrared absorption spectra, recorded during thermal treatment of the sample, formed by adsorption of C_3H_6 onto Ir_4/γ-Al_2O_3 at 298 K and 275 Torr in flowing He (A) or H_2 (B).

Table 6. H/Ir Ratios for Adsorption of Hydrogen onto Ir_4/γ-Al_2O_3 at 298 K and 104 Torr

sample	pretreatment	amt chemisorbed [mol (g sample)$^{-1}$]	H/Ir [mol/mol]
Ir_4/γ-Al_2O_3[a]	none	7.6	1.5
Ir_4/γ-Al_2O_3[a]	C_3H_6 at 298 K and 104 Torr for 0.5 h	1.0	2.0
γ-Al_2O_3 (calcined at 673 K)	none	0.3	
γ-Al_2O_3 (calcined at 673 K)	C_3H_6 at 298 K and 104 Torr for 0.5 h	0.5	

[a] 1 wt % Ir.

Table 7. Specific Adsorption Rate Parameters for Hydrogen Chemisorption on Freshly Decarbonylated and Propene-Treated[a] Ir_4/γ-Al_2O_3 at 298 K and 104 Torr[14,15]

sample pretreatment	adsorption model	total adsorption sites n_{tot} [mol g^{-1}]	adsorption rate constant k_{ads}	R^2 of fit
none	molecular	3.67×10^{-5}	1.29×10^{-4} [b]	0.72
propene[a]	molecular	1.34×10^{-4}	5.26×10^{-5} [b]	0.92
none	dissociative	7.34×10^{-5}	10[c]	0.99
propene[a]	dissociative	3.07×10^{-4}	0.18[c]	0.99

[a] Treatment at 298 K and 104 Torr for 0.5 h. [b] Units of s^{-1} $Torr^{-1}$. [c] Units of g mol^{-1} s^{-1} $Torr^{-1}$.

cm^{-1}, indicative of cluster-bound CO, which we infer was formed by the reaction of propylidyne with support oxygen.[38] The lack of formation of new infrared modes in the C−H stretching and bending frequency range as propylidyne decomposed indicates that propylidyne did not react to give dehydrogenated or polymerized species. The C_xH_y mode (1265 cm^{-1}) was unchanged when the sample was heated in flowing helium or H_2 at temperatures up to 523 K (Figures 7A,B).

Hydrogen Chemisorption Capacities of γ-Al_2O_3 and Ir_4/γ-Al_2O_3. Hydrogen chemisorption capacities[39] of γ-Al_2O_3 that had been calcined at 673 K and of Ir_4/γ-Al_2O_3 (with and without propene pretreatment) are summarized in Table 6. H_2 reacted with each sample, and samples incorporating Ir_4 took up an order of magnitude more H_2 than the support alone. The results do not distinguish between hydrogen remaining on the clusters and that which was spilled over onto the support[28] (facilitated by the Ir_4). The results indicate that propylidyne formation did not hinder the clusters' capacity to chemisorb hydrogen (the presence of propylidyne slightly increased the total amount of hydrogen chemisorbed by the sample).

Kinetics of Hydrogen Chemisorption onto Ir_4/γ-Al_2O_3. H_2 might be expected to adsorb onto Ir_4 dissociatively (as is typical for metal surfaces)[40] or molecularly.[41] These possibilities can be distinguished by the kinetics of adsorption.[14,15] The rate parameters found from the data characterizing hydrogen chemisorption onto Ir_4/γ-Al_2O_3 and onto $CH_3CH_2CIr_4/\gamma$-Al_2O_3 at 298 K and an initial H_2 pressure of 104 Torr are shown in Table 7. Parameters were determined by fitting the data to forms of the equation that correspond to each of the two modes of adsorption. The dissociative chemisorption model represents the rate data satisfactorily, whereas the molecular adsorption model does not (Table 7).[16] Dissociative adsorption kinetics are consistent with the formation of iridium hydride (Ir−H);[42] however, again we

(38) Dufour, P.; Houtman, C.; Santini, C. C.; Nédez, C.; Basset, J.-M.; Hsu, L. Y.; Shore, S. G. *J. Am. Chem. Soc.* **1992**, *114*, 4248.

(39) Hydrogen chemisorption capacities were calculated for adsorption starting at 104 Torr of H_2. H:Ir atomic ratios were calculated on the basis of the total amount of Ir.

(40) Ertl, G. *Z. Phys. Chem. N. F.* **1989**, *164*, 1115.

(41) Crabtree, R. H. *The Organometallic Chemistry of the Transition Metals*, 2nd ed.; Wiley: New York, 1994; p 64.

cannot separate hydrogen that remained on the clusters from that which spilled over onto the support.

Discussion

The data provide the first evidence of structurally well-defined supported metal clusters with hydrocarbon ligands and, thus, the opportunity to compare the formation and reactivities of these ligands on supported clusters, supported particles, and single crystals of metal. We expect the reactivity of propylidyne on Ir_4 to differ from that on extended metal surfaces, because research with gas-phase clusters[48−51] has shown that the reactivity of hydrocarbons with clusters depends sharply on the cluster size and ligand environment,[52] and because research with supported clusters has shown that the catalytic activity for arene hydrogenation depends on cluster size.[53]

Theoretical modeling of alkenes on metal surfaces[54−56] and the literature of hydrocarbon adsorbates on metal single crystals[57] show that the formation, stability, and reactivity of adsorbates on metals are sensitive to the structure and electronic properties of the metal and influenced by reaction conditions and the presence of adsorbates. We infer that, besides electronic (ligand) effects caused by the interaction of the support with the clusters, the smallness of isolated Ir_4 clusters limits what can be bonded to them, thereby restricting the reactions that can proceed on them.

In the following paragraphs, we contrast the reactivity of propene with supported Ir_4, on the one hand, and metal surfaces, on the other. We also contrast the reactivity of propylidyne formed from propene on Ir_4 with that of propylidyne on metal surfaces.

Formation of Alkylidynes on Metal Clusters and Metal Surfaces. Ethylidyne forms readily from ethene on the (111) faces of Pt[58,59] (at 255−280 K), Ir[29] (at 180 K), Pd[60] (at 300 K), and Rh[61] (at 310 K). Low-temperature (92−240 K) adsorption of ethene onto Pt(111) gives di-σ-bonded ethene, followed by conversion to ethylidyne as the temperature is increased to 280−310 K.[58,59,62] The formation of propylidyne from propene on Pt(111),[2,24,30,63] Rh(111),[23] and Pt/SiO_2[24,25] closely parallels the formation of ethylidyne from ethene on these metals.[64]

In contrast, the data presented here demonstrate that low-temperature (138 K) adsorption of propene onto Ir_4/γ-Al_2O_3 does not lead to the formation of di-σ-bonded propene[65] and then to propylidyne, but rather to the formation of C_xH_y, whereas propene adsorption at higher temperatures, 298 K, does result in the formation of propylidyne. Using density functional theory, Watson et al.[67] showed that there is a significant activation barrier (12 kJ mol^{-1}) for the transformation of π-bonded (molecularly adsorbed) ethene into di-σ-bonded ethene on the (111) face of Pt; ethene adsorbs in a π-bonded form at temperatures <50 K and transforms into di-σ-bonded ethene at higher temperatures and into ethylidyne at still higher temperatures. We suggest that the transformations of species derived from propene on Ir_4/γ-Al_2O_3 are also activated. The data show that propene remains molecularly adsorbed on Ir_4/γ-Al_2O_3 as the sample is warmed from 138 to 219 K, at which temperature it is not transformed at a significant rate into di-σ-bonded propene (and then into propylidyne) because, we suggest, the barrier for conversion of π-bonded to di-σ-bonded propene is too high.[68] However, in contrast to the reactivity of propene on Pt(111), propene molecularly adsorbed on Ir_4/γ-Al_2O_3 decomposes (to give C_xH_y) at temperatures lower than that inferred to be necessary for conversion into the di-σ-bonded species. Thus, we postulate that the reason low-temperature adsorption of propene onto Ir_4/γ-Al_2O_3 does not lead to the formation of propylidyne is that the precursor di-σ-bonded propene does not form.[70] At room temperature, propene adsorption immediately results in the formation of propylidyne; we infer that the intermediate (presumably di-σ-bonded propene) was so short-lived that we could not observe it spectroscopically.

(42) Metal hydrides have been observed on single crystals and supported particles of metal by vibrational spectroscopy.[25,43−46] Such observations are usually difficult because the peaks are often broad and weak, and we were unable to observe iridium hydrides either by infrared or NMR[47] spectroscopy.

(43) Richter, L. J.; Germer, T. A.; Ho, W. *Surf. Sci.* **1988**, *195*, L182.

(44) Candy, J. P.; Fouilloux, P.; Primet, M. *Surf. Sci.* **1978**, *72*, 167.

(45) Primet, M.; Basset, J.-M.; Mathieu, M. V. *J. Chem. Soc., Faraday Trans. 1* **1974**, *70*, 293.

(46) Baró, A. M.; Ibach, H.; Bruchmann, H. D. *Surf. Sci.* **1979**, *88*, 384.

(47) The ^1H NMR spectrum of the sample formed by reaction of H_2 with Ir_4/γ-Al_2O_3 at 760 Torr and 298 K showed conclusive resonances only for the γ-Al_2O_3 support and the rotor (Supporting Information, Figure 6). If hydride had been present, its spectrum could have been superimposed with that of either the γ-Al_2O_3 or the rotor; alternatively, the hydride resonance could have been too broad to be distinguished from the baseline.

(48) Schnabel, P.; Irion, M. F. *Ber. Bunsen-Ges. Phys. Chem.* **1992**, *96*, 1101.

(49) Kaldor, A.; Cox, D. M. *J. Chem. Soc., Faraday Trans.* **1990**, *86*, 2459.

(50) Seivers, M. R.; Jarvis, L. M.; Armentrout, P. B. *J. Am. Chem. Soc.* **1998**, *120*, 1891.

(51) Bowers, M. T.; Kemper, P. S.; von Helden, G.; Hsu, M.-T. In *Fundamentals of Gas-Phase Ion Chemistry*; Jennings, K. R., Ed.; Kluwer: Dordrecht, The Netherlands, 1991; pp 55−85.

(52) Schnabel and Irion[48] observed that Fe_n^+ clusters ($4 \le n \le 13$) are unreactive for bonding and dehydrogenation of ethane, except for $n = 4$ or 5. Formation of Fe_4H^+ rendered the cluster unreactive for bonding and dehydrogenation of ethane, but the addition of H to Fe_3^+ (forming Fe_3H^+) rendered it reactive for bonding and dehydrogenation of ethyne, although Fe_3^+ did not bind or dehydrogenate ethyne.[48]

(53) Xu, Z.; Xiao, F.-S.; Purnell, S. K.; Alexeev, O.; Kawi, S.; Deutsch, S. E.; Gates, B. C. *Nature* **1994**, *372*, 346.

(54) Neurock, M.; Pallassana, V.; van Santen, R. A. *J. Am. Chem. Soc.* **2000**, *122*, 1150.

(55) Pallassana, V.; Neurock, M. *J. Catal.* **2000**, *191*, 301.

(56) Silvestre, J.; Hoffmann, R. *Langmuir* **1985**, *1*, 621.

(57) Yagasaki, E.; Masel, R. I. *Variation in the Mechanism of Catalytic Reactions with Crystal Face*. In *Catalysis*; Spivey, J. L., Ed.; Royal Society of Chemistry: Cambridge, 1994; Vol. 11, p 163.

(58) Cregithon, J. R.; White, J. M. *Surf. Sci.* **1983**, 327.

(59) Cremer, P.; Stanners, C.; Niemantsverdriet, J. W.; Shen, Y. R.; Somorjai, G. A. *Surf. Sci.* **1995**, *328*, 111.

(60) Gates, J. A.; Kesmodel, L. L. *Surf. Sci.* **1983**, *124*, 68.

(61) Keol, B. E.; Bent, B. E.; Somorjai, G. A. *J. Chem. Phys.* **1984**, *146*, 211.

(62) Steininger, H.; Ibach, H.; Lehwald, S. *Surf. Sci.* **1982**, *117*, 685.

(63) Koestner, R. J.; Frost, J. C.; Stair, P. C.; Van Hove, M. A.; Somorjai, G. A. *Surf. Sci.* **1982**, *116*, 85.

(64) Vibrational spectra show that propene adsorption on Pt(111) proceeds at low temperature (187 K) through a di-σ-bonded species (with the C═C bond parallel to the surface), followed at higher temperatures (231−310 K) by formation of propylidyne (with the bond between the carbyne carbon and the methylene carbon oriented perpendicular to the surface).[2,30]

(65) Low-temperature (<80 K) adsorption of propene on Ir(111) leads to the formation of di-σ-bonded propene.[66]

(66) Karseboom, S. G.; Davis, J. E.; Mullins, C. B. *Surf. Sci.* **1998**, *398*, 11.

(67) Watson, G. W.; Wells, R. P. K.; Willock, D. J.; Hutchings, G. J. *J. Phys. Chem. B* **2000**, *104*, 6439.

(68) π-Bonded propene presumably transforms into di-σ-bonded propene at a higher temperature on Ir_4/γ-Al_2O_3 than that on Ir(111),[66] because the γ-Al_2O_3 support affects the clusters as a ligand in roughly the way that potassium adsorbates increase the charge density on the Pt atoms of Pt(111), thus hindering the strong σ-donation of adsorbed ethene to platinum and reducing the chemisorption bond strength.[69] Evidence of this interaction of the support with the clusters is shown by the iridium−oxygen contributions in the EXAFS data (see Tables 1 and 2).

(69) Windham, R. G.; Bartram, M. E.; Keol, B. E. *J. Phys. Chem.* **1988**, *92*, 2862.

(70) We infer that the interaction of γ-Al_2O_3 support with Ir_4 (and potentially the limited size of the Ir_4 clusters) increases the barrier for the conversion of π-bonded to di-σ-bonded propene on Ir_4/γ-Al_2O_3.

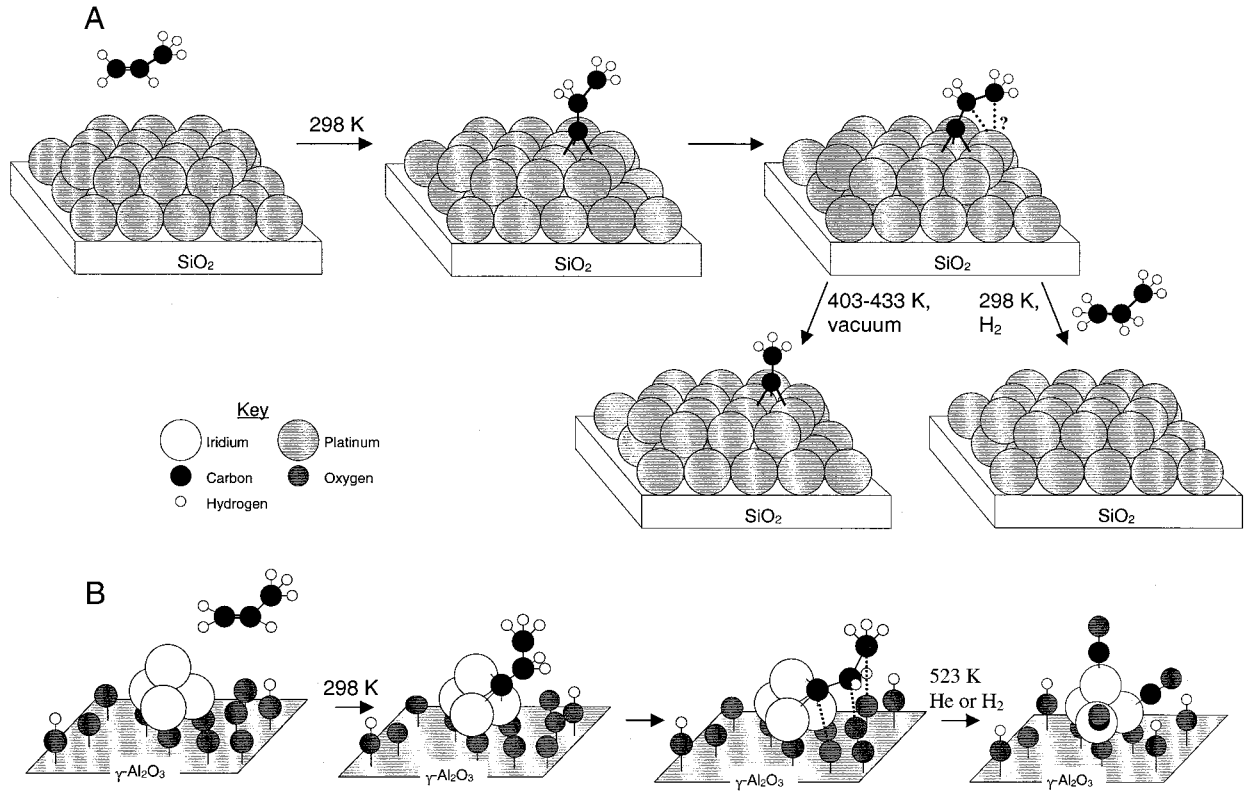

Figure 8. Schematic representation of the stability and reactivity of propylidyne on $Ir_4/\gamma\text{-}Al_2O_3$ and on extended surfaces of metal (demonstrated by particles of platinum supported on SiO_2[25]).

Not only does the temperature of adsorption affect the formation of alkylidynes from alkenes, but so does the presence of coadsorbates on the metal surface or, in our case, Ir_4 on $\gamma\text{-}Al_2O_3$. Using potassium, oxygen, bismuth, or other adsorbates, researchers[71] have demonstrated that the electronic structure and/or geometry of Pt(111) could be modified sufficiently to give a variety of surface species other than ethylidyne from the adsorption of ethene. Similarly, it has been shown[74] that preadsorption of hydrogen onto Fe(100) (forming H−Fe(100)) limits the extent of electron back-donation to coadsorbed ethene, which results in the formation of ethyl species instead of the ethynyl and methylidyne species that form on clean Fe(100).

In qualitative agreement with those results, we have found that H_2 pretreatment of $Ir_4/\gamma\text{-}Al_2O_3$ largely inhibits the formation of propylidyne from propene at 298 K, giving, instead, dehydrogenated propene. The difference in products formed from the adsorption of propene on $Ir_4/\gamma\text{-}Al_2O_3$ and H_2-pretreated $Ir_4/\gamma\text{-}Al_2O_3$ demonstrates that at least some of the adsorbed hydrogen (inferred to be hydride on the basis of the chemisorption kinetics) remained on the clusters and affected their reactivity, largely preventing the formation of propylidyne.

Thermal Decomposition of Propylidyne on Metal Clusters and Metal Surfaces. Ethylidyne on the (111) faces of Ir,[29] Rh,[75] Pt,[76] and other metals decomposes thermally to give carbonaceous products. Similarly, propylidyne decomposes thermally on Rh(111) at 270−310 K,[23] on Pt(111) at 390 K,[2] and on Pt/SiO_2 at 403−433 K.[25] At these temperatures, propylidyne gives ethylidyne on Rh(111)[23] and on Pt/SiO_2,[25] whereas it gives an unsaturated species (likely vinyl methylidyne, $M{\equiv}CCHCH_2$) on Pt(111).[2] Upon further heating, carbonaceous species similar to those formed from ethylidyne thermal decomposition are observed.

The decomposition of propylidyne on $Ir_4/\gamma\text{-}Al_2O_3$ is much different from that on extended metal surfaces. Propylidyne on Ir_4 on $\gamma\text{-}Al_2O_3$ was found to be stable in helium at temperatures as high as 523 K; at higher temperatures it reacted with the support to give CO rather than decomposing to give ethylidyne or other hydrocarbon fragments.

This sharp distinction between the reactivities of the clusters and extended metal surfaces is attributed, at least in part, to the limited size of the clusters (demonstrated by their first-shell Ir−Ir coordination number of 3) and their site-isolation (demonstrated by the lack of higher-shell Ir−Ir contributions in the EXAFS). We infer that an ensemble of metal atoms incorporating more than just the three metal atoms to which propylidyne is bonded is required for the thermal decomposition of propylidyne, as shown schematically in Figure 8A. This inference is bolstered by the work of Chakarov and Marinova,[77] who showed that as a result of preadsorption of CO onto Ir(110), ethylidyne became thermally stable at higher temperatures (∼50 °C) than when CO was absent. The authors concluded that the adsorbed CO broke up the periodic array of the surface and blocked the formation of the decomposition products, thereby increasing ethylidyne's thermal stability.[77]

By analogy, we infer that the limited size of the site-isolated Ir_4 clusters is not sufficient to allow the formation of propylidyne decomposition products; instead, at higher temperatures, the

(71) By adsorbing potassium[69,72] (or oxygen[62]) on Pt(111), Zhou et al.[72] and Windham et al.[69] (or Steininger et al.[62]) demonstrated that the reaction of ethene could be directed from that giving ethylidyne to that giving π-bonded ethene and/or di-σ-bonded ethene. Windham et al.[73] used adsorbed Bi atoms as site-blocking agents to limit the amount of di-σ-bonded ethene formed from ethene gas on Pt(111).

(72) Zhou, X.-L.; Zhu, X.-Y.; White, J. M. *Surf. Sci.* **1988**, *193*, 387.
(73) Windham, R. G.; Koel, B. E.; Paffet, M. T. *Langmuir* **1988**, *4*, 1113.
(74) Merrill, P. B.; Madix, R. J. *J. Am. Chem. Soc.* **1996**, *118*, 5062.
(75) Dubois, L. H.; Castner, D. G.; Somorjai, G. A. *J. Chem. Phys.* **1980**, *72*, 5234.
(76) Baró, A. M.; Ibach, H. *J. Chem. Phys.* **1981**, *74*, 4194.
(77) Chakarov, D. V.; Marinova, T. S. *Surf. Sci.* **1990**, *227*, 297.

propylidyne on the clusters reacts with the neighboring oxygen atoms of the support to give CO (Figure 8B).

Reactivity of H_2 with Propylidyne on Metal Clusters and Metal Surfaces. Shahid and Sheppard[25] found that a large fraction of the propylidyne and di-σ-bonded propene on Pt particles in Pt/SiO_2 was hydrogenated when the sample was exposed to H_2 at room temperature. Ogle and White[78] reported that both ethylidyne and propylidyne on Pt(111) readily exchange hydrogen with gaseous D_2 at 330 K.

In contrast, we observed that propylidyne on Ir_4/γ-Al_2O_3 does not react with H_2 at temperatures up to 523 K or undergo isotopic exchange with gaseous D_2 at 298 K. Again, we infer that the difference in reactivities between propylidyne on Ir_4/γ-Al_2O_3 and propylidyne on extended metal surfaces is related to the smallness and site-isolation of the clusters. This inference is bolstered by the results of Keol et al.,[61] who observed that the rate of H/D exchange in ethylidyne ligands on Rh(111) at 310 K depends strongly on the fraction of the metal surface that is bare. They postulated a reaction proceeding through an ethylidene intermediate (μ_2-$CDCH_3$), presumably requiring metal bonding sites neighboring those to which ethylidyne is bonded.[79] Such a process is blocked on Ir_4/γ-Al_2O_3, because there are no metal bonding sites neighboring those to which the alkylidyne is bonded.

Furthermore, because the presence of propylidyne on Ir_4/γ-Al_2O_3 did not hinder the chemisorption of hydrogen by the clusters, the lack of reactivity of propylidyne on Ir_4/γ-Al_2O_3 with H_2 or D_2 (for isotopic exchange or hydrogenation) is not caused by the lack of available hydrogen. We infer that the lack of adjacent metal sites prevents the reaction of hydrogen with propylidyne because the intermediates cannot form (Figure 8).

(78) Ogle, K. M.; White, J. M. *Surf. Sci*. **1986**, *165*, 234.

(79) The methyl H extraction/D transfer from carbene carbon to methyl carbon (resulting in the formation of μ_3-$CCDH_2$ from μ_2-$CDCH_3$) was determined to be the rate-limiting step.[61]

(80) Goursot-Leray, A.; Carles-Lorjou, M.; Pouzard, G.; Bodot, H. *Spectrochim. Acta, Part A* **1973**, *29A*, 1497.

(81) Wyckoff, R. W. G. *Crystal Structures*, 2nd ed.; Wiley: New York, 1963; Vol. 1, p 10.

(82) Trömel, M.; Lupprich, E. *Z. Anorg. Allg. Chem.* **1975**, *414*, 160.

(83) Churchill, M. R.; Hutchinson, J. P. *Inorg. Chem.* **1978**, *17*, 3528.

Conclusions

Infrared and ^{13}C NMR spectroscopy were used to characterize the formation and reactions of propylidyne on site-isolated Ir_4 clusters supported on γ-Al_2O_3. EXAFS spectra show that the Ir_4 tetrahedra remained essentially unchanged during the reactions at 298 K. H_2 chemisorption measurements provide evidence for the formation of hydride ligands on the supported clusters. Propylidyne on Ir_4/γ-Al_2O_3 is more stable and less reactive with H_2 than propylidyne on extended metal surfaces. The difference indicates the need for an ensemble of metal atoms (in addition to the three to which propylidyne is bonded) for the reaction of propylidyne. Thus, the data highlight the unique reactivity of supported (site-isolated) metal clusters, specifically demonstrating their ability to shut off reactions that occur on extended metal surfaces.

Acknowledgment. This research was supported by the National Science Foundation (Grant CTS-9617257). We thank the W. M. Keck Foundation for funds to purchase the NMR spectrometer. We acknowledge beam time and the support of the U.S. Department of Energy, Division of Materials Sciences, under Contract No. DE-FG05-89ER45384 for its role in the operation and development of beamline X-11A at the National Synchrotron Light Source. The NSLS is supported by the Department of Energy, Division of Materials Sciences and Division of Chemical Sciences, under Contract No. DE-AC02-76CH00016. We are grateful to the staff of beam line X-11A for their assistance. We acknowledge the Stanford Synchrotron Radiation Laboratory, which is operated by Stanford University for the Department of Energy, Office of Basic Energy Sciences, for access to beam time on beam line 2-3. The EXAFS data were analyzed with the XDAP software.[12]

Supporting Information Available: Table of crystallographic data. Seven figures, including infrared spectra, ^{13}C NMR and ^1H NMR spectra, and propene chemisorption as a function of time. This material is available free of charge via the Internet at http://pubs.acs.org.

JA002818Q